CIRP Annals - Manufacturing Technology 68 (2019) 547–550

Contents lists available at ScienceDirect

CIRP Annals - Manufacturing Technology

journal homepage: http://ees.elsevier.com/cirp/default.asp

Identification of machine tool squareness errors via inertial measurements

Károly Szipka [a], Andreas Archenti (2)[a,*], Gregory W. Vogl [b], M. Alkan Donmez (2)[b]

[a] Department of Production Engineering, KTH Royal Institute of Technology, Brinellvägen 68, 10044, Stockholm, Sweden
[b] Engineering Laboratory, National Institute of Standards and Technology (NIST), 100 Bureau Drive, Gaithersburg, MD 20899-8220, USA[1]

ARTICLE INFO

Keywords:
Measurement
Machine tool
Squareness error

ABSTRACT

The accuracy of multi-axis machine tools is affected to a large extent by the behavior of the system's axes and their error sources. In this paper, a novel methodology using circular inertial measurements quantifies changes in squareness between two axes of linear motion. Conclusions are reached through direct utilization of measured accelerations without the need for double integration of sensor signals. Results revealed that the new methodology is able to identify squareness values verified with traditional measurement methods. The work supports the integration of sensors into machine tools in order to reach higher levels of measurement automation.

1. Introduction

The importance of increasing productivity and quality improvement in the fabrication of complex shape components with tighter tolerances and high surface accuracy has led to the introduction of high-performance multi-axis machine tools. Machine tool axes move the cutting tool and workpiece to their desired positions for component manufacturing [1], but over a machine tool's lifetime, various errors lead to performance degradation.

One error that plays an important role for the accuracy of multi-axis machine tools, and potentially could be estimated from online metrology, is the squareness between machine tool linear axes [2]. Squareness can degrade during a machine tool's lifetime after: (i) installation of equipment, due to structural deformations of the foundation, (ii) accidental crashes during production, and (iii) years of usage under heavy-duty process induced loads. A slight error in squareness, the magnitude of which depends upon the topology of the machine, may exhibit a significant workpiece inaccuracy. ISO 230-1 [3] describes three methods to directly measure the squareness between two axes of linear motion: mechanical reference square with linear displacement sensor, reference straightedge with reference indexing table, and optical square with laser straightness interferometer. Two indirect methods to estimate the squareness are the circular test, described in ISO 230-4 [4], and the diagonal displacement test, described in ISO 230-6 [5]. Of the five methods, perhaps the most widely used is the circular test using telescoping ballbar [6]. A telescoping ballbar is relatively economical with respect to equipment, setup time, and measurement and analysis time. However, all these methods still require interruption of production by manual setup of the measuring instrument on machine tools, leading many manufacturers to forgo periodic squareness measurements.

An online circular test, based on data from an embedded inertial measurement unit (IMU), could enable periodic squareness measurements with minimal disruptions to production. Previous work has shown that an IMU-based method could detect changes in the translational and angular error motions of an individual machine axis due to axis degradation [7]. The present paper goes beyond this by introducing a novel method for characterizing multi-axis performance by detecting changes in squareness between two linear axes.

Fig. 1 outlines the approach, in which two axes of a machine tool move an IMU (Step 1) in a nominally circular motion for an

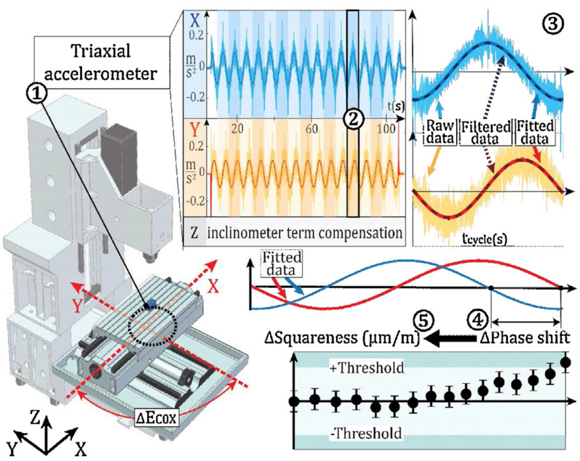

Fig. 1. Schematic view of the introduced IMU-based circular test method for monitoring changes of squareness indicating steps.1–5.

* Corresponding author.
E-mail address: archenti@kth.se (A. Archenti).
[1] Official contribution of the National Institute of Standards and Technology, not subject to copyright in the United States.

https://doi.org/10.1016/j.cirp.2019.04.070

N- number of clockwise (CW) and counterclockwise (CCW) cycles. The acceleration data from the IMU is processed (Step 2–4) to yield the change of squareness over time with the elimination of the need for displacement measurement via double integration. The yielded change of squareness can be further used with thresholding to alert the manufacturer about machine tool performance degradation (Step 5). This paper describes the methodology (Section 2), experimentation (Section 3), data analysis (Section 4), and validation and verification (Section 5) of the introduced IMU-based circular test method.

2. Methodology

The proposed method enables the robust identification of the change of squareness under industrial conditions. The main steps include the simulation of motion components, including positions, velocities, and accelerations, for both nominal and cases affected by errors (Fig. 2(a)), the implementation of tests and pre-processing of measurement data (Fig. 2(b)), and the data analysis in order to determine the squareness degradation over time (Fig. 2 (c)). Further tests with the IMU require only the implementation of part (b) and (c).

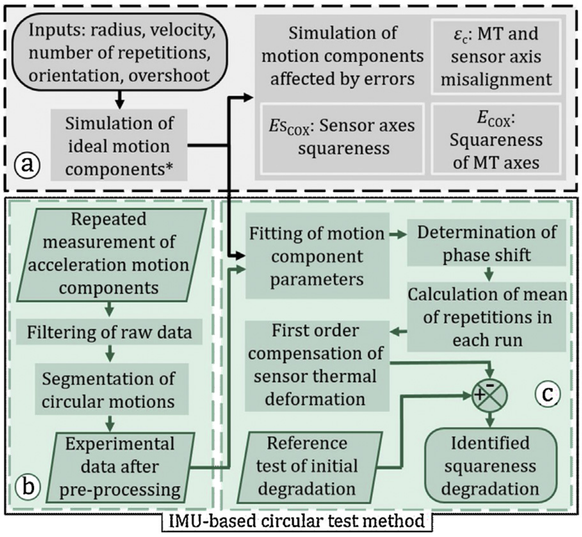

Fig. 2. Flow chart of the methodology to identify the degradation of machine tool squareness of linear axis motion.

Circular motion generated by two linear axes can be modeled as complex harmonic motion, following Lissajous formulation. The ideal accelerations in X and Y directions (a_x *and* a_y) along a circular trajectory can be described with parametric equations:

$$a_x(t) = A_x \cdot \cos(\omega_x t - \theta_x) + C_y \cdot \cos(\omega_y t + \frac{\pi}{2} - \theta_y) \quad (1)$$

$$a_y(t) = A_y \cdot \cos\left(\omega_y t + \frac{\pi}{2} - \theta_y\right) + C_x \cdot \cos(\omega_x t - \theta_x) \quad (2)$$

In the above equations, A_x and A_y are the amplitudes, ω_x and ω_y are the frequencies, and θ_x and θ_y are the phase shifts for the X and Y directions, respectively. The terms C_x and C_y are the vibration amplitudes resulting from misalignment between the sensor axes and the machine axes average motion, which can be expressed by ε_c. The relationship between the vibration amplitudes and the sensor misalignment is described in Eq. 3. Please note that the average axis motion is not known a priori.

$$\begin{bmatrix} C_x \\ C_y \end{bmatrix} = \begin{bmatrix} A_y \\ A_x \end{bmatrix} \cdot \tan(\varepsilon_c) \quad (3)$$

For a given radius and feed speed, the positions, velocities, and accelerations including ω_x and ω_y frequencies and A_x and A_y amplitudes of the accelerations, can be calculated. Then, the effects of three main error sources were considered (see Fig. 3), including:

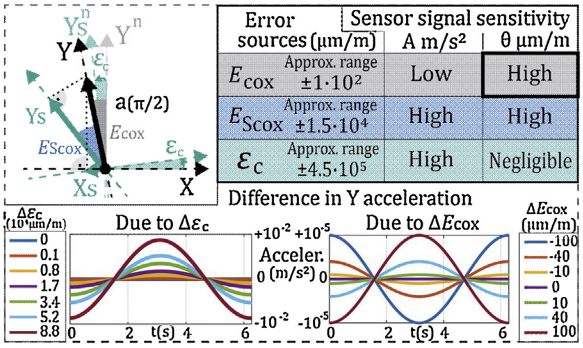

Fig. 3. Simulated main contributors affecting the reading of the sensors. Simulations were implemented for radius of 0.1 m and velocity of 0.1 m/s.

(i) ε_c, the average misalignment between the machine tool axes and the sensor axes due to setup inaccuracies (which determines C_x and C_y), (ii) E_{SCOX}, the squareness of sensor axes, and (iii) E_{COX}, the squareness of the machine tool average axes, which is the actual measurand.

Traditionally, homogenous transformation matrices (HTMs) are used to express the effects of these error sources on commanded positions. Taking the programmed feed speed into account, the time-dependent nominal positions are used as input to the HTMs to calculate corresponding time-dependent actual positions. Through differentiations, the effect of alignment errors can be derived on time-dependent acceleration. The calculated accelerations can then be related to the amplitude and phase-shift parameters in Eqs. (1) and (2). Insertion of Eq. (3) into Eqs. (1) and (2) yields expressions for the X- and Y-accelerations that depend on ε_c misalignment. This relation of the amplitudes can also be confirmed through time-dependent HTMs.

The squareness error results in two sinusoids for $a_x(t)$ and $a_y(t)$ with a phase difference between the two . This confirms the analogy with the Lissajous curve, where the varying phase shift changes the aspect ratio of the resulting ellipse. Elliptical shape of the 'circular' position trajectory is widely accepted as the quantifiable characteristic of the squareness error between the two linear axes [6]. The sensitivity between the error sources and the parameters of the accelerometer signals can be seen in Fig. 3, as well as the simulated effect of alignment errors on acceleration amplitudes.

An important implication of the simulations is that the phase shift is attributed with E_{COX} (measurand) and E_{SCOX} (where X and Y are directions of a right-handed Cartesian coordinate system):

$$E_{COX} + E_{SCOX} = \theta_y - \theta_x \quad (4)$$

The limitation is that the separation of the machine tool and the sensor axes squareness is difficult. However, if the latter can be regarded as constant, then the change of squareness is reasonably attributed with the change of squareness of the machine tool axes. Thus, after a reference test of the initial condition of the machine tool, the change in the phase shift for repeated tests characterizes squareness degradation. Furthermore, the simulated magnitudes of the misalignment ε_c, which are realistic for the given alignment procedure, were found to negligibly affect the phase shift. This helps enable the phase shift of the acceleration signals to be a robust indicator for squareness. As shown in Fig. 2, important steps related to filtering of raw data and proper fitting of acceleration motion component parameters have to be implemented to detect values of θ_x and θ_y. These steps are further described in the data analysis section (Section 4).

3. Experimentation

Tests were performed under industrial conditions on a three-axis machine tool with axis traverse ranges of X:1000 mm, Y:510 mm, and Z:561 mm, see Fig. 4. The kinematic chain of the

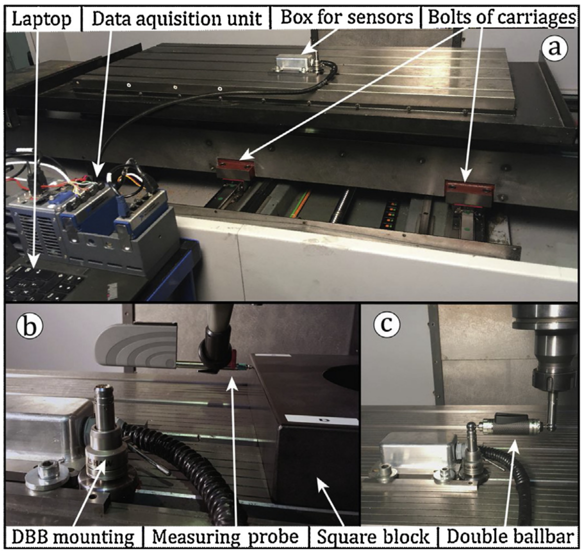

Fig. 4. Experimental setup: (a) overall test setup, (b) square block measurement (c) V&V measurements with telescoping ballbar.

machine is [t-(C)-Z-b-Y′-X′-w] where X and Y axes are stacked to represent the motion of the table.

Six levels of squareness error, including the reference, were induced by mechanically changing the relation between X (upper) and Y (lower) axes (marked later as Ref. and D1-D5 in Figs. 6 and 7). The procedure to change and measure squareness was performed as follows: (1) mechanically loosen the bolts that connect the carriages of the X and Y axes; (2) apply an external load to push the X axis out of its orientation with respect to Y, while keeping the Y axis fixed; (3) tighten bolts with a torque wrench; and (4) measure the induced squareness with a square block (SB) and a telescoping ballbar (DBB). The SB and DBB data were used for validation and verification (V&V) purposes (see Section 5).

The measurement system contains a sensor box with a triaxial accelerometer, a mount for the sensor box, and a data acquisition unit. The selection of sensors is crucial to reduce test uncertainty. The chosen accelerometer has a bandwidth of 0–300 Hz (corresponding to the half-power point), a nominal sensitivity of 2000 mV/g, and a noise output of 7 μg rms/ $\sqrt{Hz}$. The maximum value of the cross-axis sensitivity is 3%, which defines an upper bound estimate for the squareness E_{SCOX}. The box, including the accelerometers, was clamped in the middle of the X and Y axes and roughly aligned along the T-slots of the table.

Sensor data is collected while circular trajectories are executed by the synchronized motion of two linear axes. The circular trajectories include repeated CCW and CW directions which are executed subsequently. For each of the six levels of squareness error, acceleration data was collected for 155 runs, each composed of 30 cycles (15 CCW and 15 CW cycles). To have stable measurement conditions, an 180° overshoot at the beginning and end of each CCW or CW motion was implemented. This minimized transient vibrations for sufficient dynamic stability of the repeated cycles.

Various radii and feed rates can be selected for the test method. However, it is important that in order to maximize the signal-to-noise ratio, a higher speed (resulting in higher accelerations) is desired. At the same time, the machine should be able to perform the trajectories with stability and without significant effects of the inertial forces. For tests in this paper, a nominal radius of 0.1 m and a feed of 0.1 m/s was selected.

4. Data analysis and convergence

The measured accelerations are first pre-processed in order to prepare the dataset for fitting of harmonic motion components and determination of phase shift between the fitted X and Y accelerations. The pre-processing starts with the filtering of raw data, which is essential for detecting spatial frequencies relevant for squareness error. A first-order low-pass Butterworth filter (zero-phase) was used, with a cutoff frequency of 4 Hz. The cutoff frequency was selected to be sufficiently high in order to reasonably capture squareness, but low enough to prevent the sensitivity of the output quantity on other spatial frequencies. In other words, 4 Hz was selected through iterations during analysis of cutoff frequencies above 1 Hz, which is greater than the fundamental motion frequency of approximately 0.167 Hz. The last step in the pre-processing is the segmentation of repeated circular trajectories implemented in each run (see Steps 2–3 in Fig. 1). After the segmentation, the acquired signals can be investigated without any change in the phase shift of the signals, but at the same time the effect of drift is minimized. Drift occurs when data is compared from a longer time interval. Drift was an important optimization criterion for the selection of a higher test speed to reduce the test duration.

After pre-processing, CW and CCW data is averaged in order to eliminate the effect of servo controller mismatch. Before that, however, the CW dataset has to be flipped in order to match corresponding positions with the CCW (positive) direction. As servo mismatch has a similar distortion effect as squareness on a circular trajectory, therefore the acquisition of CW and CCW data is essential to separate the different sources. In the next step the acceleration data is fitted according to the motion component parameters defined in Eqs. (1) and (2) with an additional constant term. The fit is implemented in two steps in order to yield θ_x, θ_y and C_y, C_x quantities. First, the first terms of Eqs. (1) and (2) are fitted to the filtered measurement data with known frequency (0.167 Hz) to solve for A_x, A_y, θ_x, and θ_y. Second, the second terms of Eqs. (1) and (2) are fitted to the residuals of the previous fit and C_y and C_x are determined. With known amplitudes through Eq. (3), a mean for ε_c can be deduced (which in this experiment was identified to be 2.1°).

The sine-wave-fit technique is considered as one of the most powerful tools for phase difference measurement [8]. A least-squares method was applied with bisquare weights for both fits. The application of robust fitting is important as peaks (due to the reversal of axes) can corrupt the results (see Fig. 5). The composed fitting strategy is the result of an optimization, which was implemented through observing the convergence of the mean and standard deviations of test data via different fitting strategies. For each run, a mean value of the repeated cycles is calculated. With this approach, the double integration to time-dependent position is avoided, which has important advantages to reduce the effect of noise during the quantification of squareness.

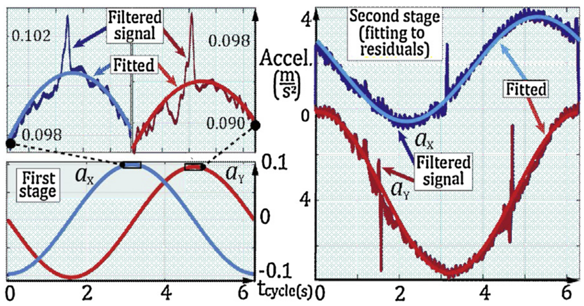

Fig. 5. Implemented fitting strategy in case of one cycle of a run.

The convergence of the mean values with increasing number of runs is essential in order to improve the quality of the characterized squareness and also to evaluate the quality of the implemented fits. For the implemented experiments, the convergence for all six cases (one reference case and five degradations) is demonstrated in Fig. 6.

The test uncertainty can be further reduced by the compensation of linear thermal deformation of the accelerometer. In the case of starting up measurements, the electronics of the sensors generate heat, resulting in a thermal deformation and in a slight

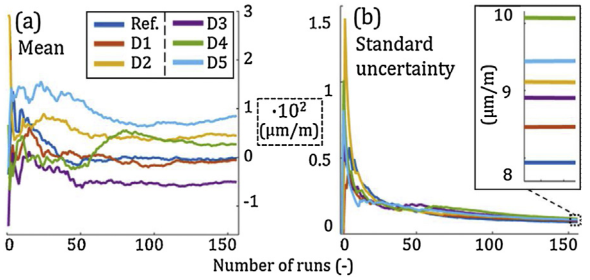

Fig. 6. Convergence of (a) mean and (b) type A standard uncertainty of the change in squareness for the reference condition and 5 degradation stages.

change of squareness between the two sensor axes (E_{SCOX}). This affects the characterization of the squareness as it is directly coupled with E_{COX} (through Eq (3). This phenomenon was reduced by proper warm up of the sensor itself before measurement, and by compensation with the application of a first-order regression.

5. Validation and verification

As Fig. 4 shows, two standardized measurement approaches were used for V&V purposes. The SB was used to increase control over mechanical error inducement, and the DBB was selected as the second instrument because it is capable of measuring under similar conditions as the performed accelerometer-based tests (same radius of circle and feed).

Ten repeated measurements were implemented both before and after error inducement, and the effect of warm up of the machine on the squareness was also investigated and found to be negligible. Fig. 7 shows significant agreement between results of the IMU-based circular test and results of the two standardized tests. Thus, the introduced method is able to identify squareness value changes verified with the traditional measurement methods. Type A standard uncertainties of the IMU-based results are the outcome of convergence (for 155 runs), as seen in Fig. 6(b). The V&V is limited by the differences in the principles of the approaches. Furthermore, tests could not be performed at the very same positions in the work volume of the machine tool, resulting in an estimated difference of 2 µm/m–4 µm/m between the IMU- and the standard-based results.

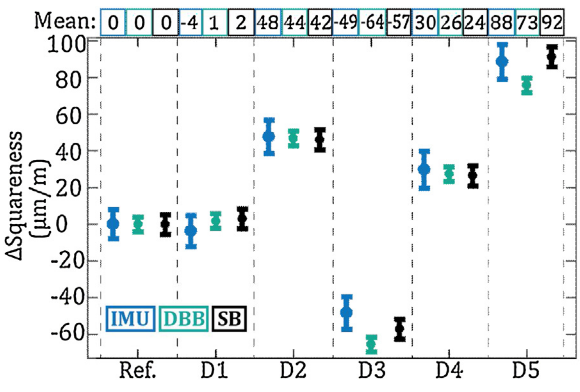

Fig. 7. Comparison between the different methods for quantification of the change of squareness values for six different experimental conditions (from reference to the five different levels of degradations). Error bars correspond to $k = 1$ and mean values are given in a unified 1 µm resolution.

6. Conclusions and discussions

The squareness of multi-axis machine tools is directly linked to the quality of machined components. A novel methodology is proposed in this paper to identify the change in squareness between machine tool linear axes. The procedure is based on inertial measurements in which triaxial accelerometer data is collected while the sensor moves along circular trajectories executed by the synchronized motion of two stacked linear axes. The methodology includes pre-processing of measurement data and data analysis to determine the squareness degradation over time.

The proposed method was experimentally verified and validated under industrial conditions on a three-axis machine tool by comparing squareness values quantified by the proposed IMU-based method with those from a conventional square block and telescoping ballbar. Results were well confirmed; measured mean values overlap as shown in Fig. 7 (with a coverage factor of $k = 1$). The convergence of the mean value of the measurement quantity can be reached with the introduced approach. As the IMU can be integrated within a machine tool (eliminating the need for setup time), and it can be directly applied as a warm up cycle, valuable production time can be saved, in comparison with other existing approaches.

The presented integration of sensors in advanced production equipment can facilitate the development of measurement automation towards the concept of self-diagnostics of machine tools. By integrating the data acquisition and analysis in the machine tool controller, compensation for process planning and optimization of maintenance can be performed by monitoring the change of squareness through periodic online measurements.

References

[1] Altintas Y, Verl A, Brecher C, Uriarte L, Pritschow G (2011) Machine Tool Feed Drives. *CIRP Annals — Manufacturing Technology* 60(2):779–796.
[2] Schwenke H, Knapp W, Haitjema H, Weckenmann A, Schmitt R, Delbressine F (2008) Geometric error measurement and compensation of machines—An update. *CIRP Annals — Manufacturing Technology* 50(2):660–675.
[3] ISO 230-1 (2012) *Test Code for Machine Tools — Part 1: Geometric Accuracy of Machines Operating under No-Load or Quasi-Static Conditions*, International Organization for Standardization, Geneva, Switzerland.
[4] ISO 230-4 (2005) *Test Code for Machine Tools — Part 4: Circular Tests for Numerically Controlled Machine Tools*, International Organization for Standardization, Geneva, Switzerland.
[5] ISO 230-6 (2002) *Test Code for Machine Tools — Part 6: Determination of Accuracy of Positioning on Body and Face Diagonals (Diagonal Displacement Tests)*, International Organization for Standardization, Geneva, Switzerland.
[6] Kakino Y, Ihara Y, Nakatsu Y, Okamura K (1987) The Measurement of Motion Errors of NC Machine Tools and Diagnosis of Their Origins by Using Telescoping Magnetic Ball Bar Method. *CIRP Annals — Manufacturing Technology* 36(1):377–380.
[7] Vogl GW, Donmez MA, Archenti A (2016) Diagnostics for Geometric Performance of Machine Tool Linear Axes. *CIRP Annals — Manufacturing Technology* 65 (1):377–380.
[8] Sedlacek M, Krumpholc M (2005) Digital Measurement of Phase Difference – a Comparative Study of DSP Algorithms. *Metrology and Measurement Systems* 7 (4):427–448.